is quite good for $h/b \geq 0.4$, but the data curve and deviate at low filling.

The curvature in the experimental data can be explained by the presence of higher order modes not considered in the analysis. These modes would be expected to have more influence for thicker and higher dielectric-constant loads. The Teflon dielectric, while rather thick, had a relatively low dielectric constant. An experiment with a glass slab, having a relatively higher dielectric constant and being relatively thick, showed the same trend but exhibited even more curvature. Deviations from theory, especially at low filling, may also be due to the slot through which the dielectric entered the waveguide. This would influence the propagation even when the top of the dielectric was flush with the waveguide wall, and thus, experimentally, $h/b=0$ does not truly represent the empty waveguide.

Summary

A simple two-mode approximation is presented for the computation of the phase shift of a vane-type dielectric loaded waveguide. This analysis considered the coupling of the TE_{10} and TM_{11} empty waveguide modes by the dielectric. Experimental results tended to support the conclusion that the two-mode analysis is adequate for relatively thin and relatively low dielectric-constant loads centered in the waveguide. The formulation given in (3) can be used to calculate the propagation constant for off-center loads [6] also. However, the accuracy of a two-mode solution using the TE_{10} and TM_{11} modes could be expected to deteriorate rapidly as the load moved off center and other modes became important. A lossy dielectric slab such as used in vane-type attenuators can also be accommodated by this analysis [3].

References

[1] W. E. Hord and F. J. Rosenbaum, "Approximation technique for dielectric loaded waveguides," *IEEE Trans. Microwave Theory Tech.*, vol. MTT-16, pp. 228–233, Apr. 1968.
[2] S. A. Schelkunoff, "Generalized telegraphists' equations for waveguides," *Bell Syst. Tech. J.*, vol. 31, pp. 784–801, July 1952.
[3] R. M. Arnold and F. J. Rosenbaum, "Nonreciprocal wave propagation in semiconductor loaded waveguides in the presence of a transverse magnetic field," *IEEE Trans. Microwave Theory Tech.*, vol. MTT-19, pp. 57–65, Jan. 1971.
[4] R. H. Sheikh and M. W. Gunn, "Wave propagation in a rectangular waveguide inhomogeneously filled with semiconductors," *IEEE Trans. Microwave Theory Tech.* (Corresp.), vol. MTT-16, pp. 117–121, Feb. 1968.
[5] S. C. Kashyap and M. A. K. Hamid, "Perturbation analysis in dielectric loaded waveguides," *Electron. Lett.*, vol. 5, pp. 140–141, Apr. 3, 1969.
[6] A. S. Vander Vorst, A. A. Laloux, and R. J. M. Govaerts, "A computer optimization of the Raleigh-Ritz method," *IEEE Trans. Microwave Theory Tech.*, vol. MTT-17, pp. 454–460, Aug. 1969.

A Single-Tuned Oscillator Circuit for Gunn Diode Characterizations

P. W. DORMAN

Abstract—**A Gunn diode oscillator circuit with predictable performance has been developed based on a concept already shown to be practical with IMPATT diodes. Frequency jumps, multifrequency output, and tuning difficulties are eliminated without sacrificing circuit efficiency. The circuit is quite versatile and well suited for Gunn diode characterizations.**

An oscillator circuit first developed for *X*-band IMPATT diode characterization [1] has been adapted for use with Gunn diodes. The predictable single-tuned type of behavior obtained with IMPATT diodes [2], [3] has now been achieved with Gunn diodes as well without sacrificing circuit efficiency. This short paper reports the circuit configuration.

The Gunn oscillator circuit is illustrated in Fig. 1. The diode is mounted in the center conductor of a coaxial transmission line which is coupled to the side wall of a $\lambda_g/2$ waveguide cavity. This coaxial line is terminated in its characteristic impedance beyond the cavity. A $\lambda/4$ series choke is included between the cavity and termination to minimize power leakage into the termination. The external load is coupled to the cavity by a rotary joint–iris combination that allows smooth coupling variation between a value dictated by the iris dimensions and zero coupling. Mode suppressors are located on the

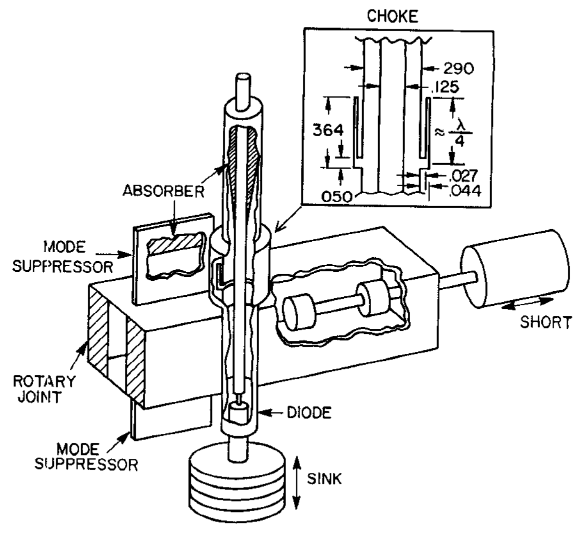

Fig. 1. Gunn oscillator circuit.

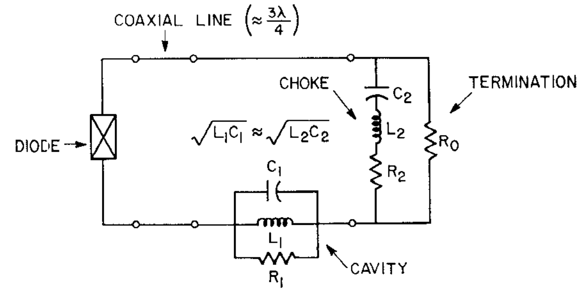

Fig. 2. Equivalent circuit.

broad walls of the cavity to eliminate mode probabilities (notably TE_{201}) other than the desirable TE_{101} [4].

Near cavity resonance, the equivalent circuit of the oscillator is shown in Fig. 2. With the reference plane located on the coaxial line at the center of the waveguide height, the loaded cavity is represented by a parallel resonant circuit. Without the choke in place the impedance versus frequency at this plane can be plotted on a Smith chart as a circular impedance locus which lies on the real axis between the center and right side of the chart. As seen from the diode position, this resonant loop can be positioned anywhere around the chart by varying the length of coaxial line between the diode and the cavity. The frequency of this resonance is easily varied by the waveguide short, while the diameter of the resonant loop is changed with the variable coupling between cavity and load. Thus almost any impedance value can be presented at the diode terminals in a predictable manner while properly terminating the diode at other frequencies. For diode impedance characterizations this tuning ability is sufficient.

For maximum output power under optimum tuning conditions, the wasted power due to the absorber in series with the cavity is unacceptable. By adding a choke in the coaxial line $\lambda/4$ from the effective cavity terminals, we can greatly reduce the termination resistance over a limited range of frequencies. In the case of IMPATT diodes, a choke is not necessary. The impedance of ordinary IMPATT diodes is quite small ($\approx 1\ \Omega$); therefore, light cavity loading plus proper phasing gives the required impedance at the diode terminals, cavity impedance R_1 remains high compared to R_0, and most of the power is coupled to the cavity. Gunn diodes, however, have a rather high impedance ($\approx 10\ \Omega$); the cavity must be heavily loaded reducing R_1 so the choke is needed to reduce power loss to the termination R_0. With the dimensions shown in the insert of Fig. 1, the choke has a Q of approximately 100, an effective series resistance of 7 Ω, and the single-tuned behavior of the oscillator circuit is well preserved. The effect of the choke is clearly seen from Fig. 3, which shows the maximum output power versus frequency for a constant diode bias. At

Manuscript received December 9, 1971; revised February 10, 1972.
The author is with Bell Telephone Laboratories, Inc., Murray Hill, N. J. 07974.

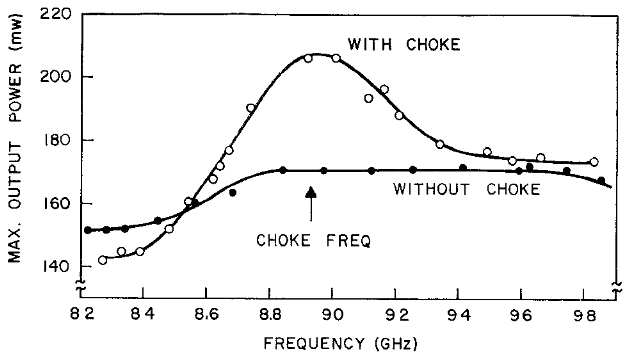

Fig. 3. Output power versus frequency.

the design frequency of the choke, the output power of that diode was improved by 20 percent over the corresponding case without the choke in place. The difference in the curves at the band edges is due to a nonoptimum electrical length between cavity and choke.

The behavior of this circuit is well understood and the circuit is now being used as an analytical tool for measuring the actual Gunn diode impedance. By simply scaling the dimensions, however, it seems well suited for various system applications as well.

References

[1] F. M. Magalhaes and K. Kurokawa, "A single-tuned oscillator for IMPATT characterizations," *Proc. IEEE* (Lett.), vol. 58, pp. 831–832, May 1970.
[2] N. D. Kenyon, "A circuit design for MM-wave IMPATT oscillators," in *Int. Microwave Symp. Dig.*, pp. 300–303, 1970.
[3] K. Kurokawa and F. M. Magalhaes, "An X-band 10-watt multiple-IMPATT oscillator," *Proc. IEEE* (Lett.), vol. 59, pp. 102–103, Jan. 1971.
[4] P. W. Dorman, "Gunn diode impedance measurements using a single-tuned oscillator," *Int. Microwave Symp. Dig.*, pp. 150–151, 1971.

The Accuracy of AM and FM Noise Measurements Employing a Carrier Suppression Filter and Phase Detector

JOSEPH L. FIKART, JAN NIGRIN, AND PAUL A. GOUD

Abstract—**The accuracy of a commonly used noise-measuring system at microwave frequencies is calculated under actual measuring conditions. Serious deviations are shown to occur, which impose a lower and upper frequency limit on "double-channel" AM and FM noise measurements, respectively.**

In laboratory systems for measurement of the AM and FM noise of microwave oscillators, the basic circuit shown in Fig. 1 is often used [1]–[4]. If the switch SW-1 is positioned such that only channel I is in operation, the circuit works as an ordinary AM detector (with the detector diodes D1 and D2 connected in phase). When both channels are used and the detector diodes are switched in opposition, the hybrid tee-diode combination operates as a phase detector and, in conjunction with the carrier suppression filter in channel II, forms a frequency discriminator for FM measurements. This "double-channel" mode of operation can also be used (at least theoretically) for AM measurements, as suggested in the literature [2], [4].

The operation of this circuit and its calibration have so far been described in terms of assumed "ideal" conditions; namely, the hybrid tee is perfect, the cavity is tuned precisely to the carrier frequency of the RF signal, and the cavity input impedance is perfectly matched at that frequency, thus producing no reflection of the carrier. The purpose of this short paper is to show how measurement accuracy is influenced in the actual case, where neither of the above criteria is satisfied.

Manuscript received December 20, 1971; revised April 17, 1972. This work was supported by the National Research Council of Canada under Grant A3725.
The authors are with the Department of Electrical Engineering, University of Alberta, Edmonton, Alta., Canada.

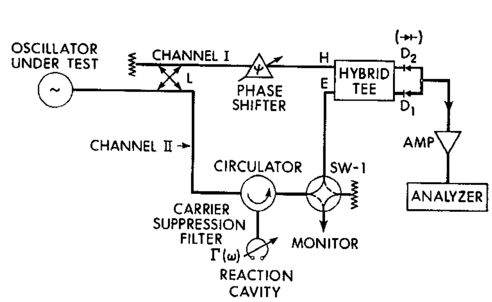

Fig. 1. Basic AM and FM noise-measuring system.

The input signal can be mathematically expressed as follows:

$$v(t) = \mathrm{Re}\,\{V_c[1 + m(t)] \exp [\omega_c t + \phi(t)]\} \tag{1}$$

where $m(t)$ and $\phi(t)$ stand for the amplitude and phase noise modulation, respectively. With $m(t) \ll 1$, $\phi(t) \ll \pi/2$, and assuming $m(t)$, $\phi(t)$ to be truncated sample functions of wide-sense stationary processes [5], the Fourier spectrum of $v(t)$ becomes [6]

$$v(\omega) = \frac{1}{2}[V_c\delta(\omega - \omega_c) + V_c^*\delta(\omega_c + \omega)] + \frac{V_c}{2}[m(\omega - \omega_c) + j\phi(\omega - \omega_c)] + \frac{V_c^*}{2}[m^*(\omega + \omega_c) - j\phi^*(\omega + \omega_c)] \tag{2}$$

where δ is the Kronecker delta and $m(\omega) = \phi(\omega) = 0$ for $\omega \geq \omega_c$. The asterisk denotes a complex conjugate.

According to Fig. 1, the oscillator signal $v(t)$ gets to the detector diodes via two channels. The RF voltage spectrum at the respective diodes is

$$v_{D1}(\omega) = v(\omega)[Le^{j\psi} + \Gamma(\omega)] \tag{3}$$

$$v_{D2}(\omega) = v(\omega)[Le^{j(\psi+\gamma)} - (1 - A)\Gamma(\omega)] \tag{4}$$

where L is the coupling into channel I (see Fig. 1), γ is the phase inaccuracy of the hybrid tee (typically 2°), and A is the power-division imbalance of the hybrid tee (typically 0.01). The reflection coefficient $\Gamma(\omega)$ of the cavity is given by [4]

$$\Gamma(\omega) = \left(\frac{\beta - 1}{2} - jQ_0\frac{\omega - \omega_0}{\omega_0}\right)\left(1 + jQ_0\frac{\omega - \omega_0}{\omega_0}\right)^{-1} \tag{5}$$

where β is the cavity coupling parameter and ω_0 is its natural resonant frequency.

It can be shown by inspecting (2) that the equivalent AM noise modulation of an RF signal can be obtained from its sidebands and carrier by

$$m(\omega_m) = v(\omega_c + \omega_m)/V_c + v^*(\omega_c - \omega_m)/V_c^*. \tag{6}$$

Assuming linear detection, the Fourier component at ω_m of the balanced detector output voltage then is

$$V(\omega_m) = k\{\,|c_1|\,m_{D1}(\omega_m) - |c_2|\,m_{D2}(\omega_m)\} \tag{7}$$

where c_1 and c_2 are the carrier components at diodes 1 and 2, respectively, obtained from (3) and (4) for $\omega = \omega_c$. The quantities $m_{D1}(\omega_m)$ and $m_{D2}(\omega_m)$ are obtained by applying (6) on the signal represented by (3), (4).

In the ideal case, the power spectral density $V_s(\omega_m)$ of (7) is given by

1) $\psi = 90°$

$$V_{s1}(\omega_m) = \Delta\Omega_s(\omega_m)(\omega_m^2 + \omega_0^2/Q_0^2)^{-1} \tag{8}$$

2) $\psi = 0°$

$$V_{si}(\omega_m) = m_s(\omega_m)(\omega_m Q_0/\omega_0)^2(1 + \omega_m^2 Q_0^2/\omega_0^2)^{-1} \tag{9}$$

where $\Delta\Omega_s(\omega_m) = \phi_s(\omega_m)\omega_m^2$ and $m_s(\omega_m)$, $\phi_s(\omega_m)$ are the power spectral densities of the AM and FM modulations. These relations are plotted in Fig. 2.

In practical measurement setups, conditions differ significantly from the ideal ones. In good systems, the hybrid tee asymmetry is within the limits indicated above, the cavity reflection at ω_c may be